JOURNAL OF MATERIALS SCIENCE 22 (1987) 1419–1431

Growth of selenium thin films

M. ÖZENBAŞ*
Department of Metallurgical Engineering, Middle East Technical University, Ankara, Turkey

Quantitative measurements of the formation and growth of selenium films on sapphire, glass, aluminium and nickel substrates have been made for various substrate temperatures (T) and evaporation times (t) using a scanning electron microscope (SEM). The film formation and growth process was thought to be a mechanism of the adsorption of impinging selenium atoms on the stable clusters, and the growth of these clusters as evaporation continues. The difference in the values of the activation energies for the growth of selenium on different substrates was explained by considering them as apparent energies which contain the adsorption, desorption, surface diffusion and binding energy terms. The experimental results also indicated an increase in the re-evaporation of adatoms from the substrates at higher temperatures.

1. Introduction

In recent years, some significant progress has been made toward a better understanding of the mechanism of nucleation and growth of thin films due to their potential applications, especially to the technology of electronic devices. Several theoretical approaches to this problem are given in the literature [1–27]. However, among the studies reported in the literature, only a few have been concerned with the relation between the growth of selenium films and its kinetics on different substrates [17, 22, 25].

Selenium photoreceptors are used primarily for the photoreproduction of documents. These photoreceptors are vacuum deposited films of amorphous selenium (a-Se) on conductive substrates, and the electrical, optical and mechanical properties of selenium are unique in their application to photocopying. Thin a-Se films are most commonly prepared by the condensation of selenium atoms from the vapour phase. At the earliest stage, atomistic condensation takes place which forms three dimensional nuclei. These nuclei then grow and form a continuous film by diffusion controlled processes.

The aim of the present work was to study the growth phenomena of selenium films on different substrates as a function of substrate temperature and evaporation time and to present the details of phenomena which may be responsible for the present experimental findings.

2. Experimental details

Four different types of substrate materials were used for the deposition of selenium films: non-corrosive glass slides, sapphire, aluminium (vacuum deposited on glass), and nickel (vacuum deposited on glass). Glass slides and sapphire substrates were cleaned ultrasonically using trichlorethylene, acetone, and ethyl alcohol before the deposition takes place. All the substrates thus prepared were, however, exposed to the atmosphere before selenium coating took place.

A filament-wound alumina boat was used for vacuum evaporation of selenium to minimize any reactions between the source material and selenium. Selenium pellets pressed from Merck chemical-grade powder (99.5% Se, 0.005% Pb and 0.005% Fe) were used for deposition in a vacuum of 4×10^{-6} torr. The substrates were coated in groups of four in the coating unit (Nanotech, Microprep 300-S, Nanotech Ltd., Manchester, UK) to ensure the same temperature conditions for a selected evaporation time.

The substrate temperatures were varied by using a heater that consisted of a copper block in which a resistance wire is wound on a marble piece. The marble was isolated from the copper block by mica sheets. A copper plate with countersunk holes was the substrate holder. A copper-constantan thermocouple placed near the substrates was used to measure the substrate temperature (T) within $\pm 2°C$. A shutter mounted between the evaporation source and the substrates allowed the selenium to be melted and outgassed without contamination of the substrate.

All the samples were coated with a thin gold film to obtain a conducting surface before the microexamination of the specimen surfaces using a SEM (Cambridge Stereoscan S4-10). The observations aimed at determining the number and the size of the islands on a unit area on the film. The contact angle measurements were also carried out in the SEM by tilting the specimens 90° in order to see the islands in elevation.

3. Results and discussion

The stages of deposition during the growth of selenium films on sapphire, glass, aluminium and nickel substrates are shown in the SEM photographs in Figs 1–2, 4–6, 8–10 and 12–13, respectively. The number density n (cm^{-2}) of selenium particles was calculated for different evaporation times and substrate temperatures. The results are given in Tables I–IV and time dependence of these number densities

Present address: Max-Planck-Institut für Metallforschung, Institut für Physik, Heisenbergstrasse 1, 7000 Stuttgart 80, FRG.

0022–2461/87 $03.00 + .12

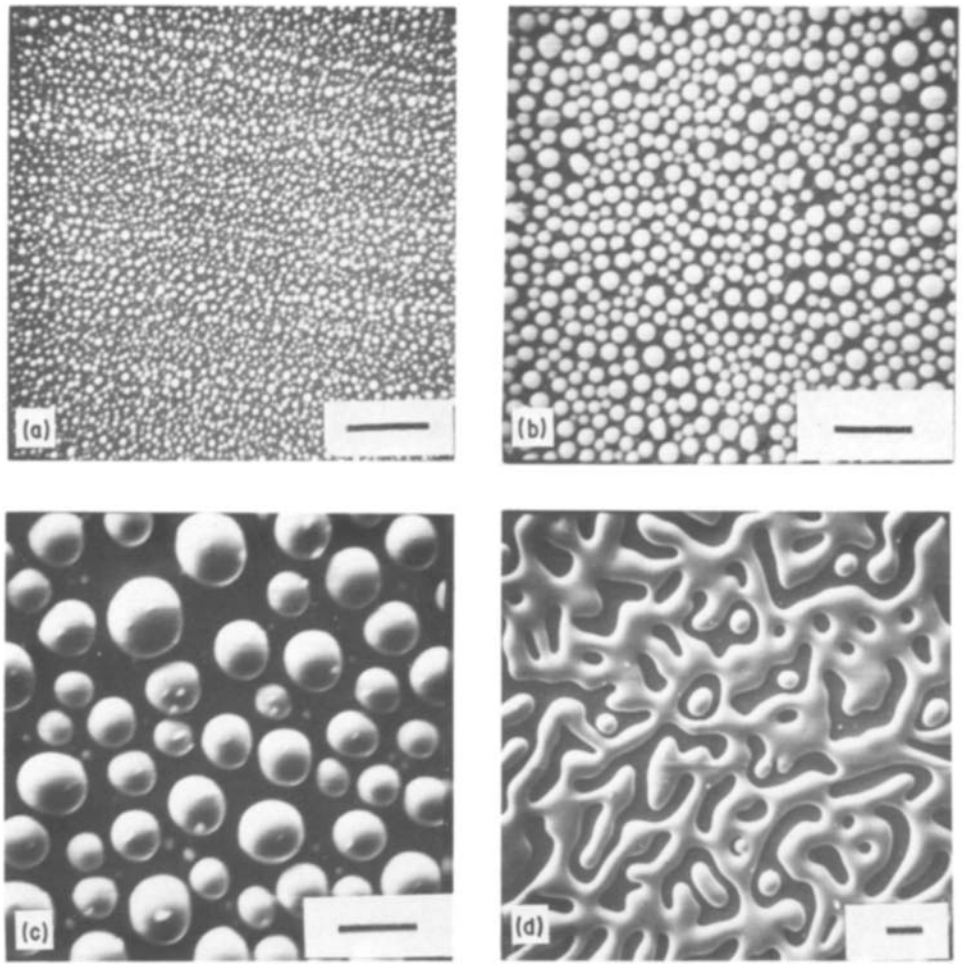

Figure 1 The growth sequence of selenium films on a sapphire substrate at the substrate temperature T of 60° C. (a) Evaporation time t, 20 sec; (b) 50 sec; (c) 100 sec; (d) 200 sec. Scale bar, 2μm.

are shown in Figs 3, 7, 11 and 14. Obvious features of these curves are the decrease in the number density of selenium particles with time. As can be seen qualitatively from the scanning electron micrographs, number density n also decreases with decreasing substrate temperature T for a fixed evaporation time.

It is clear that particles of dimensions smaller than the resolution limit of the SEM could not be counted. In practice, even the particles slightly larger than this limit could not be detected due to the shadowing of the greater particles. The smallest island diameters measured in the initial growth stages of the present study were about 10 nm in diameter.

The formation and growth of thin selenium films can be characterized by four stages. Firstly, the nucleation of random, three dimensional, isolated critical nuclei at an initial deposition, and their growth with further deposition forming the observable islands as shown in Figs 1a–2a, 4a–6a, 8a–10a and 12a–13a. The process is very rapid and predominantly occurs by surface diffusion. The number of islands mainly depends upon the activation energies for diffusion and adsorption of adatoms on the substrate [28]. Secondly, with further growth, the islands coalesce and if some areas are left vacant, the secondary nucleation takes place and they also grow with coalescence in the same way as primary islands. The secondary nucleated islands can be seen in Figs 1c, 2c, d, 4c, 5c, d, 6c, 8c, 12c and 13d, surrounding the primary islands. Thirdly, large scale coalescence takes place, forming a network structure. This structure can be seen in Figs 1d, 4d and 12d. Finally, elongated channels in the network structure fill up. This process is very slow and requires a considerable amount of the deposit to form a continuous film.

Several processes contribute to the growth of

TABLE I Time dependence of the number density n (cm^{-2}) × 10^7 of selenium particles on a sapphire substrate

Substrate temperature (° C)	Evaporation time (sec)			
	20	50	100	200
60	29.12	10.20	2.72	2.21
70	54.44	14.42	4.96	3.73
80	*	16.32	11.34	3.00
100	*	*	7.12	–

*No condensation is observed using the SEM.

TABLE II Time dependence of the number density n (cm^{-2}) × 10^7 of selenium particles on a glass substrate

Substrate temperature (° C)	Evaporation time (sec)			
	20	50	100	200
60	27.68	8.81	4.79	3.39
70	74.66	10.49	5.44	2.42
80	*	24.78	12.06	1.51
100	*	*	2.39	–

*No condensation is observed using the SEM.

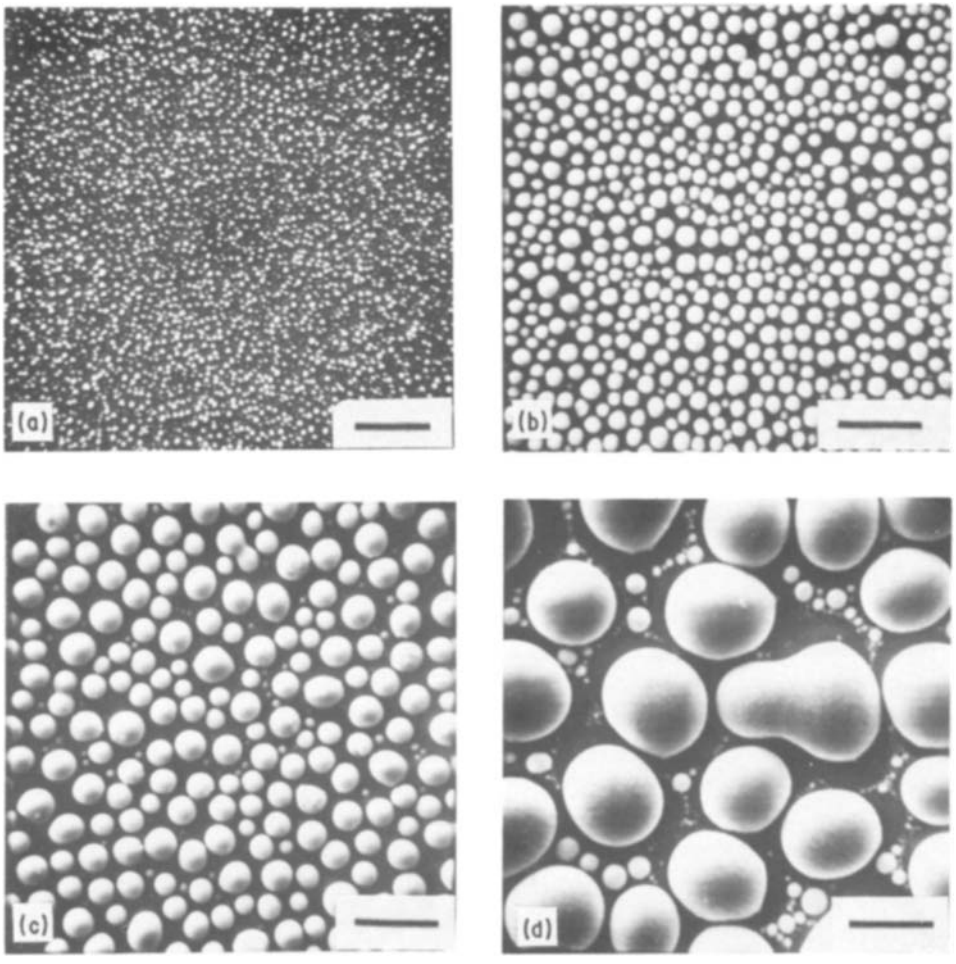

Figure 2 The growth sequence of selenium films on a sapphire substrate at $T = 70°$ C. (a) $t = 20$ sec (b) 50 sec; (c) 100 sec; (d) 200 sec. Scale bar 2.5 μm.

selenium films. Single atoms can diffuse across the substrate to join stable clusters, or they can impinge directly on the growing clusters and become incorporated into them. The most obvious observation obtained from the present experiments is that two islands which grow into each other will coalesce into one (Figs 1d, 2d, 4d, 6c, 8c, 9c, 12d and 13d). If the islands themselves are mobile, this process can happen at an earlier stage of growth.

In order to obtain quantitative information on the experimentally observed growth process, the size histograms of selenium films were obtained by measuring the sizes of the islands on each selenium film. The diameters of the coalesced islands were calculated by assuming that they are composed of two hemispherical islands. The volumes of some of the films were not calculated due to the fact that they consisted of irregularly shaped islands, possibly arising from the large scale coalescence. As pointed out before, some films had a network structure which affected both the calculation of island diameters and the counting of the number density of islands. The information available from the histograms, however, can only be gained by simultaneously considering a complete series of such distributions belonging to successively varying deposition times. The first feature of the histograms is that the island diameter increases as evaporation continues, showing the simultaneous growth of the islands during evaporation as shown in Fig. 15. The second piece of information obtained from the histograms is the decrease of the island size as the temperature increases, as can be seen in Fig. 16. Another important point is the presence of a peak in the small diameter range which is observed to decrease as the temperature increases.

The three dimensional form of the islands was

TABLE III Time dependence of the number density n (cm^{-2}) $\times$ 10^7 of selenium particles on an aluminium substrate

Substrate temperature (° C)	Evaporation time (sec)			
	20	50	100	200
60	39.36	13.00	3.52	2.55
70	75.95	16.72	11.35	2.02
80	*	27.35	12.22	4.70
100	*	*	8.65	–

*No condensation is observed using the SEM.

TABLE IV Time dependence of the number density n (cm^{-2}) $\times$ 10^7 of selenium particles on a nickel substrate

Substrate temperature (° C)	Evaporation time (sec)			
	20	50	100	200
60	26.71	12.37	3.17	5.51
70	93.70	39.15	7.19	4.41
80	*	57.67	35.86	12.80
100	*	*	1.46	–

*No condensation is observed using the SEM.

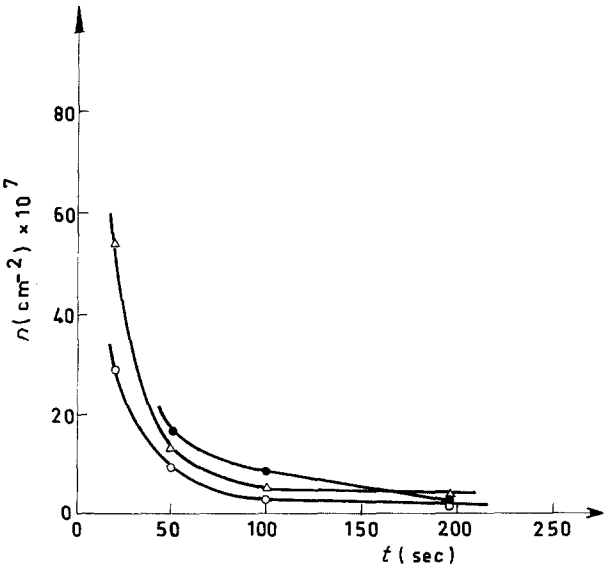

Figure 3 Time dependence of the number density n of selenium particles on a sapphire substrate for different substrate temperatures. T = ○, 60; △, 70; ●, 80° C.

assumed to be hemispherical (Fig. 17). The volume of the islands per unit area was determined for each selenium film by using the size histograms. The details of the calculations are given in [29]. Time dependence of the volume per unit area of selenium films on glass and aluminium substrates is given in Figs 18 and 19, respectively. The same values of the volume of each film were also plotted against substrate temperature in Fig. 20.

These results enable us to explain the processes during the formation and growth of selenium films on different substrates. The number density n (cm^{-2}) decreases with increasing evaporation time, as can be seen from Figs 3, 7, 11, and 14. This indicates that the atoms are sufficiently mobile to move on the substrate surface and be incorporated into other islands, giving rise to the growth of the islands. Large, somewhat irregular islands are believed to be coalesced islands. This fact can also be seen on the size histograms of selenium films by the increase in the island diameter as evaporation continues (Fig. 15). Although it was not possible to observe the islands which are smaller than the resolution limit of SEM, the increase in the volume of the films with increasing evaporation time shows that this increase is caused by the continuous adsorption of atoms from the vapour phase.

The growth sequence of selenium films on different substrates shows that bridging occurs for films at low substrate temperatures for 200 sec evaporation time, but it is not observed at higher temperatures. This is attributed to the increased mobility of atoms at higher temperatures, resulting in a reduced tendency for trapping in interstices between islands and the re-evaporation of atoms from the surface. The decrease in the average island diameter with increasing

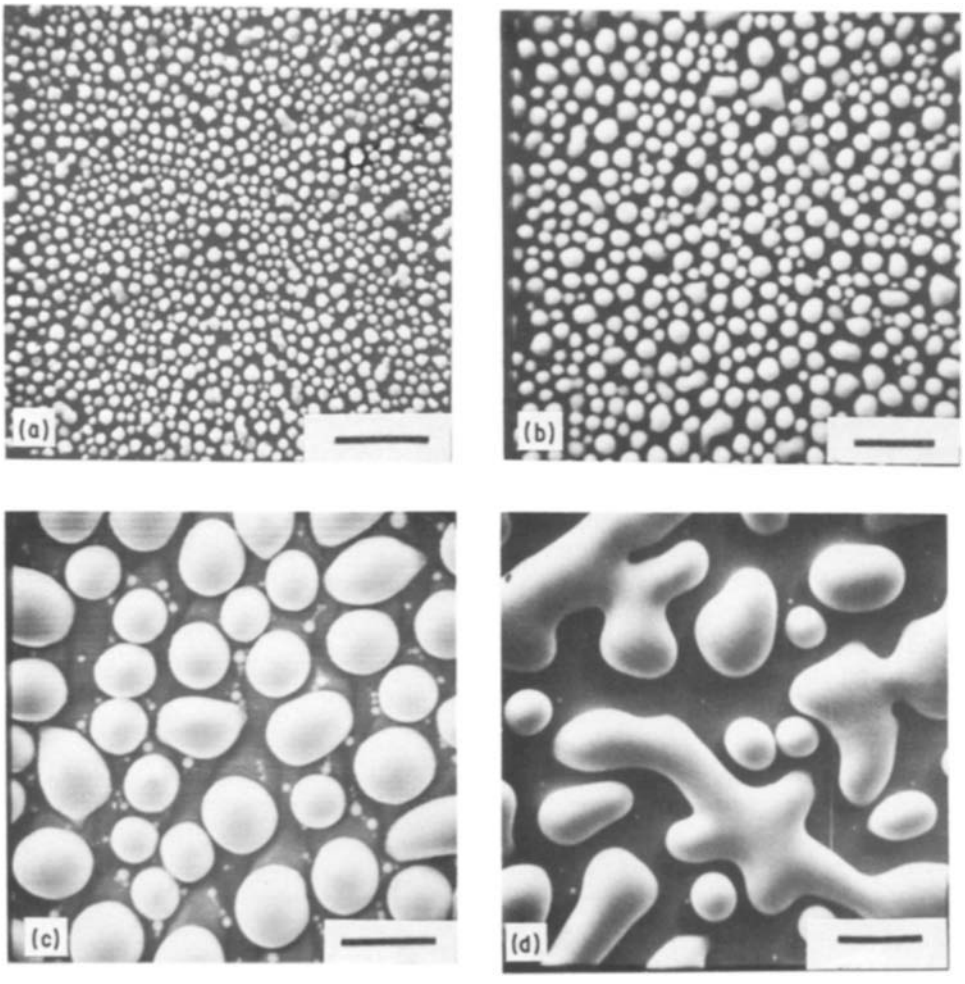

Figure 4 The growth sequence of selenium films on a glass substrate at T = 60° C. (a) t = 20 sec; (b) 50 sec; (c) 100 sec; (d) 200 sec. Scale bar 2.5 μm.

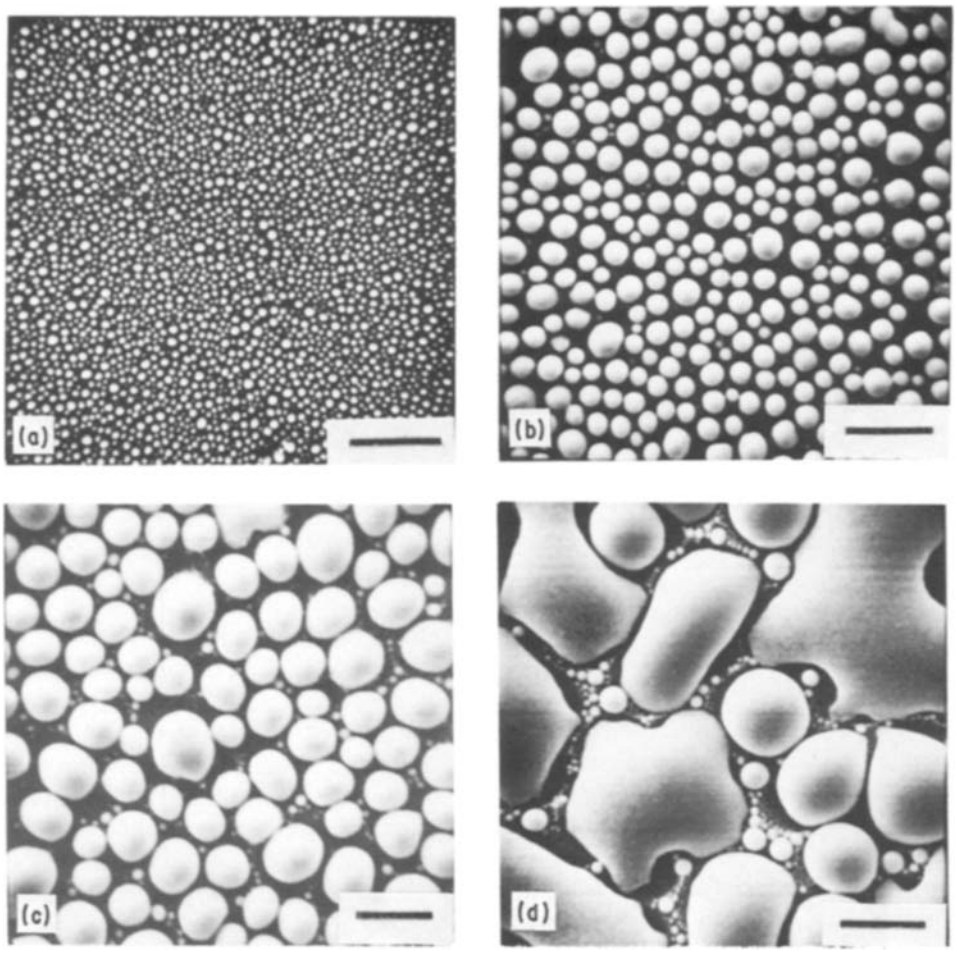

Figure 5 The growth sequence of selenium films on a glass substrate at $T = 70°$ C. (a) $t = 20$ sec; (b) 50 sec; (c) 100 sec; (d) 200 sec. Scale bar, 2.5 μm.

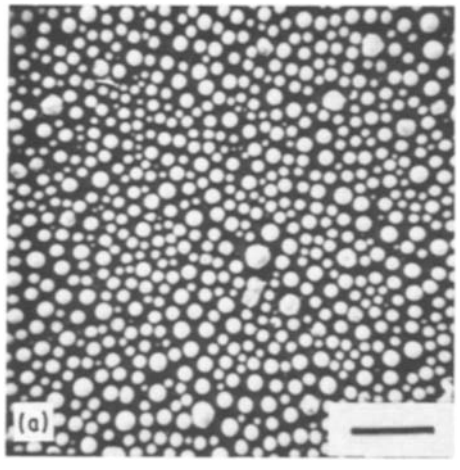

temperature (Fig. 16) together with the decrease in the volume of the films as temperature increases (Fig. 20) demonstrates that there is some re-evaporation from the substrates.

In the initial stages of condensation, islands of various sizes are in metastable equilibrium with adsorbed atoms. As these islands grow, they deplete the surrounding region of adsorbed atoms, so that further island formation is not possible in this region (called a capture zone). New islands are only formed outside the capture zone of growing islands, leading to

Figure 6 The growth sequence of selenium films on a glass substrate at $T = 80°$ C. (a) $t = 50$ sec; (b) 100 sec; (c) 200 sec. Marker represents 2.5 μm.

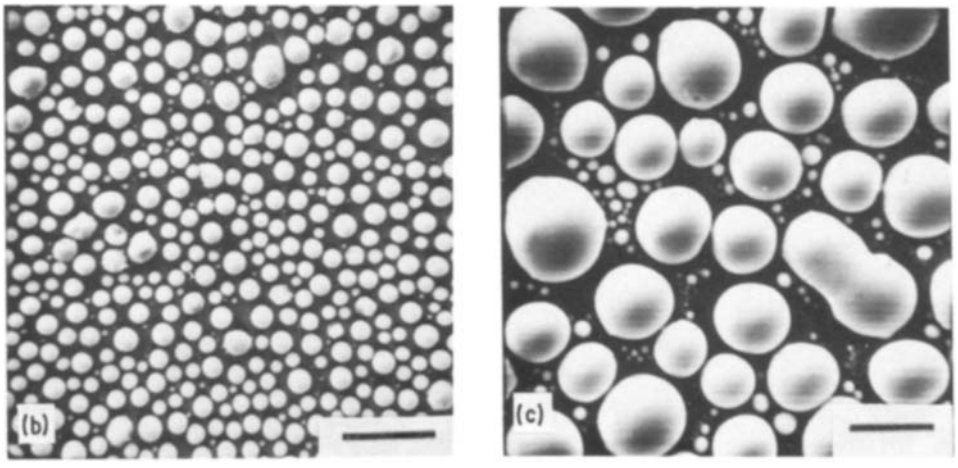

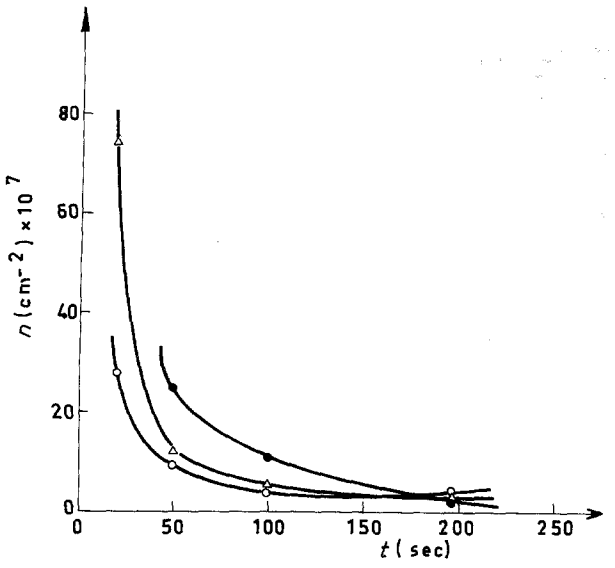

Figure 7 Time dependence of the number density n of selenium particles on a glass substrate for different substrate temperatures. T = ○, 60; △, 70; ●, 80° C.

secondary nucleation and growth processes [30]. For a constant substrate temperature, the increase in the volume of the films and the presence of the small diameter peaks on the histograms can be explained in this manner.

The deposition flux R (atoms/unit area/unit time) was taken as a constant throughout the experiments. The following equation can be written for n_{ad}, if the number of atoms impinging on the substrate for a certain evaporation time t is taken as n_{ad}

$$n_{ad} = R\left[A(t)\exp\left(-\frac{\Delta G_{s-a}}{kT}\right) + B(t)\exp\left(-\frac{\Delta G_{a-a}}{kT}\right)\Big|_{t<t_0} + C(t)\exp\left(-\frac{\Delta G_{a-a}}{kT}\right)\Big|_{t>t_0} + D(t)\exp\left(-\frac{\Delta G_{des}}{kT}\right)\right] \quad (1)$$

where ΔG_{s-a} is the activation free energy for the adsorption of atoms on the substrate surface, ΔG_{a-a} is the activation free energy for the adsorption of atoms on the adsorbed layer, and ΔG_{des} is the activation free energy for the desorption process. $A(t)$, $B(t)$, $C(t)$, and $D(t)$ are all functions of time. The first term of the above equation represents the adsorption of selenium atoms on the substrates. If one assumes that all the adsorption sites on the substrate surfaces are occupied by the impinging selenium atoms, the volume of the first layer of the selenium islands can be calculated by using the number of adsorption sites and the size histograms of each film. Details of the calculations are given in [29]. There exists a considerable difference, in the order of 10^3, between the total volume and the volume of the first layer of these films. Therefore, the first term of Equation 1 was neglected. The second term in the same equation represents the adsorption of selenium atoms on the selenium layer before t_0, where t_0 is the time required for the whole coverage of the substrate surface by the selenium layer. In the same way, the third term represents the adsorption process after t_0, where all the surface is covered by a selenium film and the process is merely in the form of depositing layers of selenium on the first monolayer. The SEM photographs showed that the adsorption process in the present study was not due to the formation of layers of selenium on the substrate surfaces, rather it was a process of forming islands of various sizes. Thus, the third term of Equation 1 was also neglected. The last term in that equation takes into account the

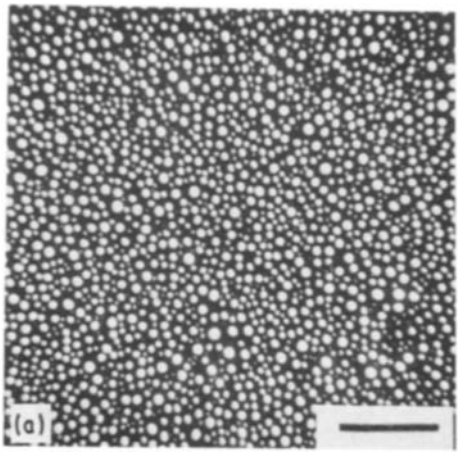

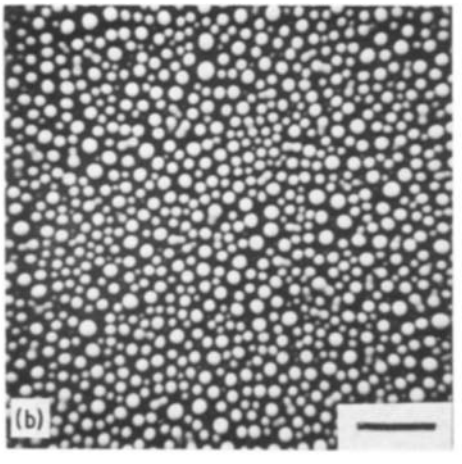

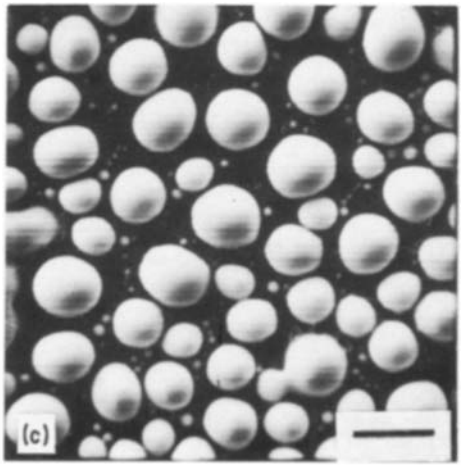

Figure 8 The growth sequence of selenium films on an aluminium substrate at T = 60° C. (a) t = 20 sec; (b) 50 sec; (c) 100 sec. Scale bar, 2.5 μm.

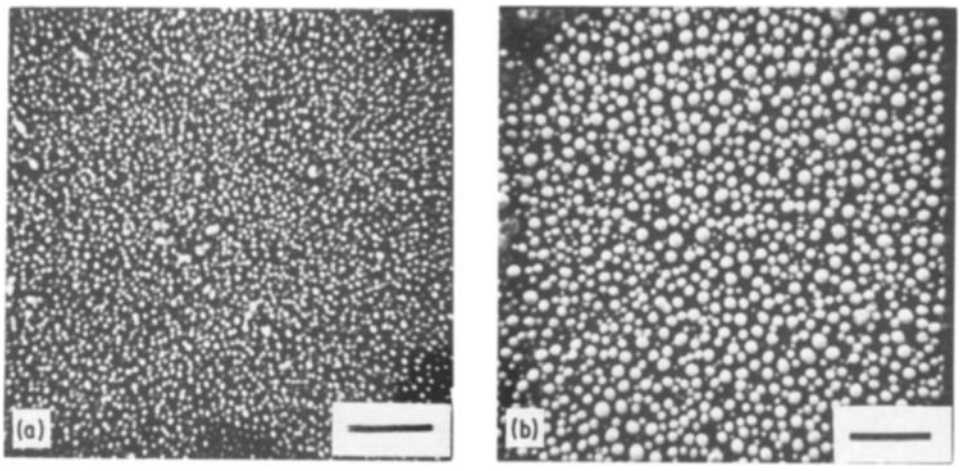

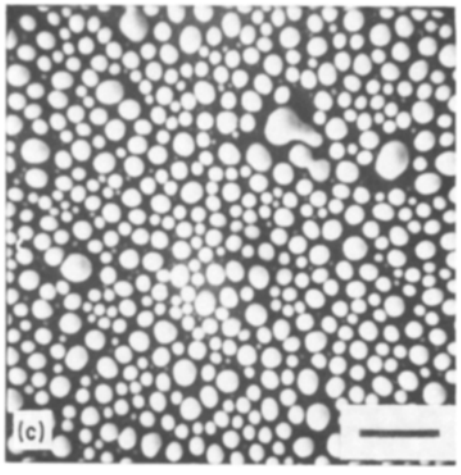

Figure 9 The growth sequence of selenium films on an aluminium substrate at $T = 70°$ C. (a) $t = 20$ sec; (b) 50 sec; (c) 100 sec. Scale bar, 2.5 μm.

process of desorption. However, the desorption of aggregates into monomers is negligible and this fourth term can also be neglected [27].

Thus, the governing equation for the volume of sel- using the relation $n_{ad} = V/v$, where v is the atomic volume

$$V = C \exp\left(-\frac{\Delta G_{apparent}}{kT}\right) f(t) \qquad (2)$$

where $\Delta G_{apparent}$ is the apparent energy of activation for the growth of selenium islands on the substrates, $f(t)$ is a function of time and C is a constant. The activation energy of the process was named as an apparent energy, because it takes into account four different energies operating in the growth process.

$$\Delta G_{apparent} = \Delta G_{ad} + \Delta G_{des} + \Delta G_{d} + \Delta G_{b} \qquad (3)$$

where ΔG_{ad} is the surface adsorption energy, ΔG_{des} is the desorption energy, ΔG_{d} is the surface diffusion energy, and ΔG_{b} is the binding energy between two adsorbed atoms.

To obtain these apparent energies on different substrates, the calculated values of the film volumes for different evaporation times were fitted to Equation 2

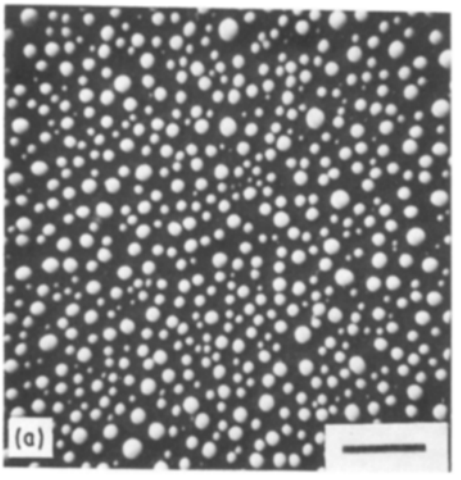

Figure 10 The growth sequence of selenium films on an aluminium substrate at $T = 80°$ C. (a) $t = 50$ sec; (b) 100 sec; (c) 200 sec. Scale bar, 2.5 μm.

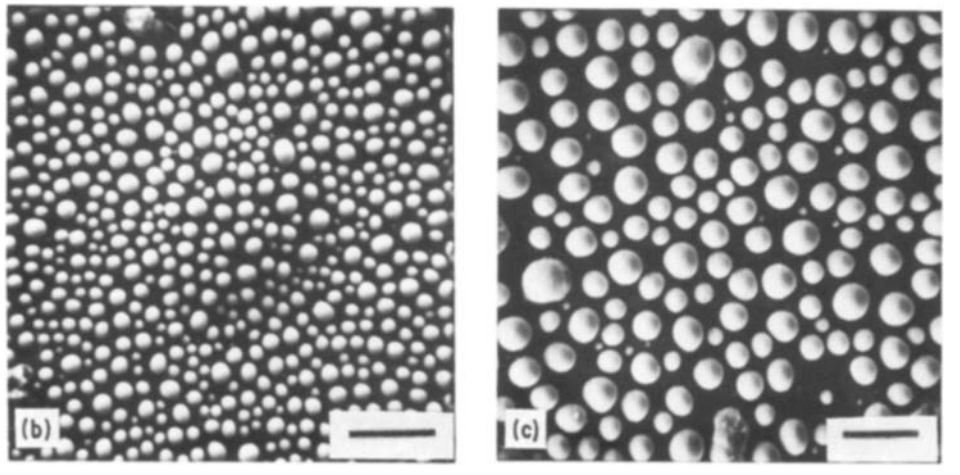

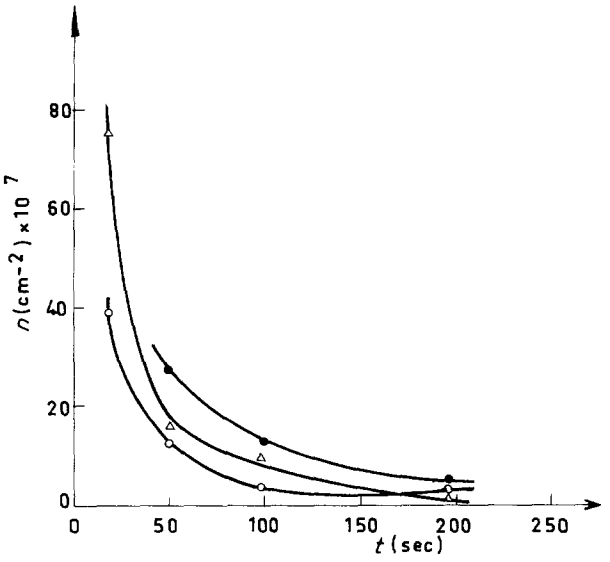

Figure 11 Time dependence of the number density n of selenium particles on an aluminium substrate for different substrate temperatures. ○, 60; △, 70; ● 80° C.

by using a computer program. The resulting equations are given in Table V for different substrates. The exponents of the exponential terms for a specific substrate were plotted against reciprocal absolute temperature and the slopes of these least-square lines were calculated. The apparent energies obtained from the slopes are given in Table VI. They are in good agreement with previous experimental results [31].

The difference in the apparent energies appears to be a good measure of the apparent surface energies, since it contains the binding energy term between the substrate and the incident selenium atoms. When the apparent energies for aluminium and nickel substrates are compared with the Pauling–Gordy electronegativity differences, it is seen that there exists a direct proportionality between the apparent energies (1.96 eV and 1.12 eV for aluminium and nickel substrates, respectively) and the electronegativity differences (0.9 and 0.6 for Al–Se and Ni–Se, respectively. Although Pauling–Gordy electronegativity differences give only an estimate of the binding energies between the atoms, the observed relationship between these values and the apparent energies shows the effect of different substrates on the growth of selenium films. The comparatively high value for the glass substrate (2.20 eV) is probably due to high microscopic surface roughness of this substrate which would impede surface diffusion, leading to an increase in the apparent energy.

The time dependency of Equation 2 was found as t^2 for each substrate, as seen in Table V. This t^2 dependence of the volume of selenium films can be explained by the smaller adsorption energy of selenium on selenium islands than that on the substrates. Thus, it can be said that the film formation and growth process

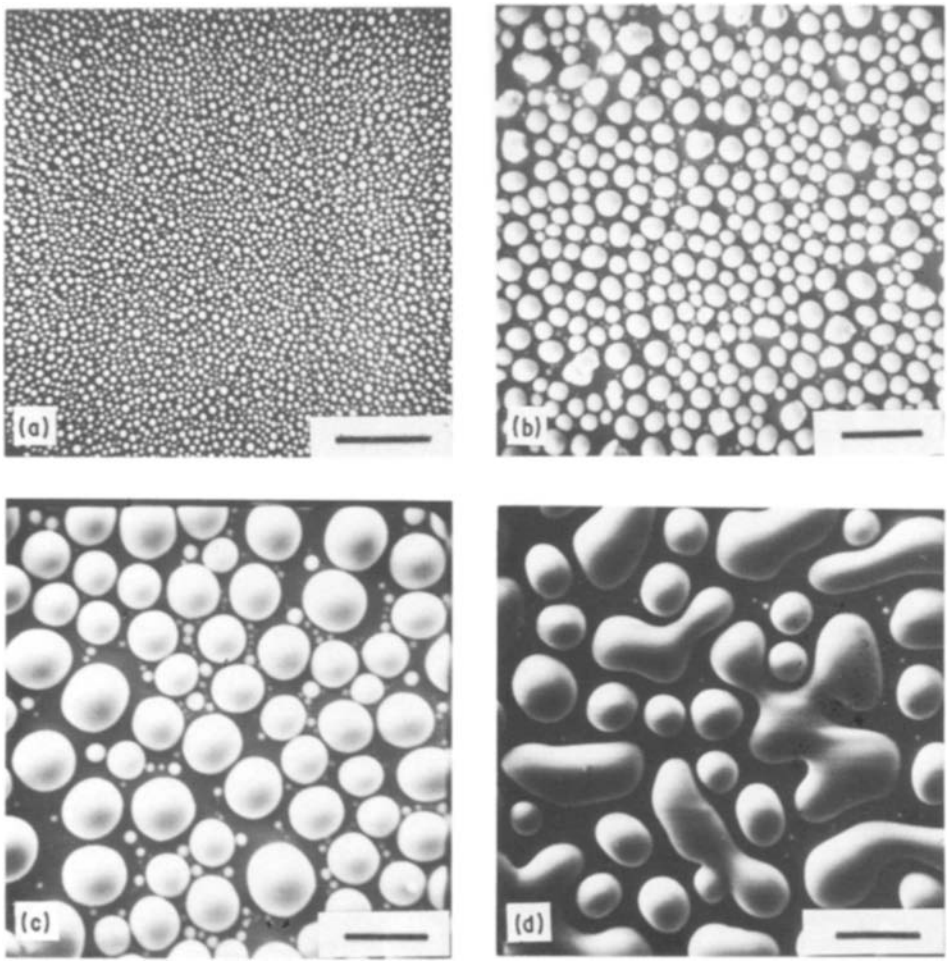

Figure 12 The growth sequence of selenium films on a nickel substrate at $T = 60°$ C. (a) $t = 20$ sec; (b) 50 sec; (c) 100 sec; (d) 200 sec. Scale bar, 2.5 μm.

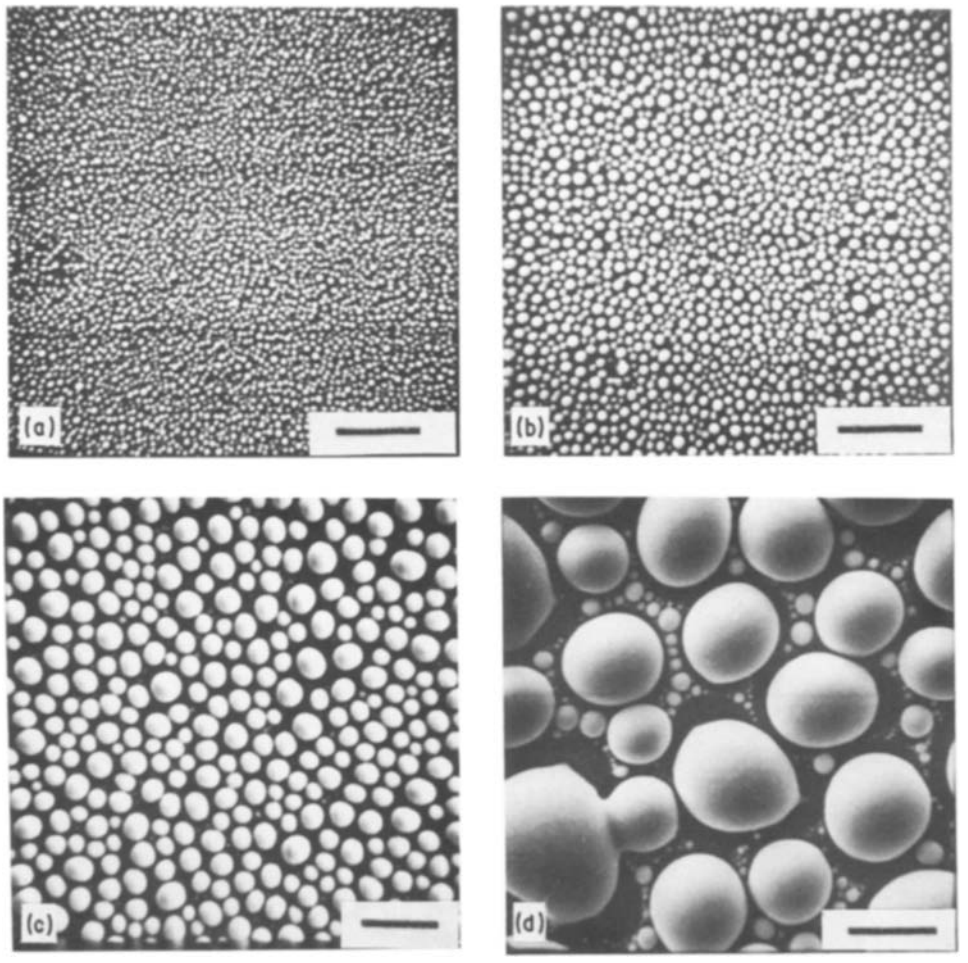

Figure 13 The growth sequence of selenium films on a nickel substrate at $T = 70°$ C. (a) $t = 20$ sec; (b) 50 sec; (c) 100 sec; (d) 200 sec. Scale bar, 2.5 μm.

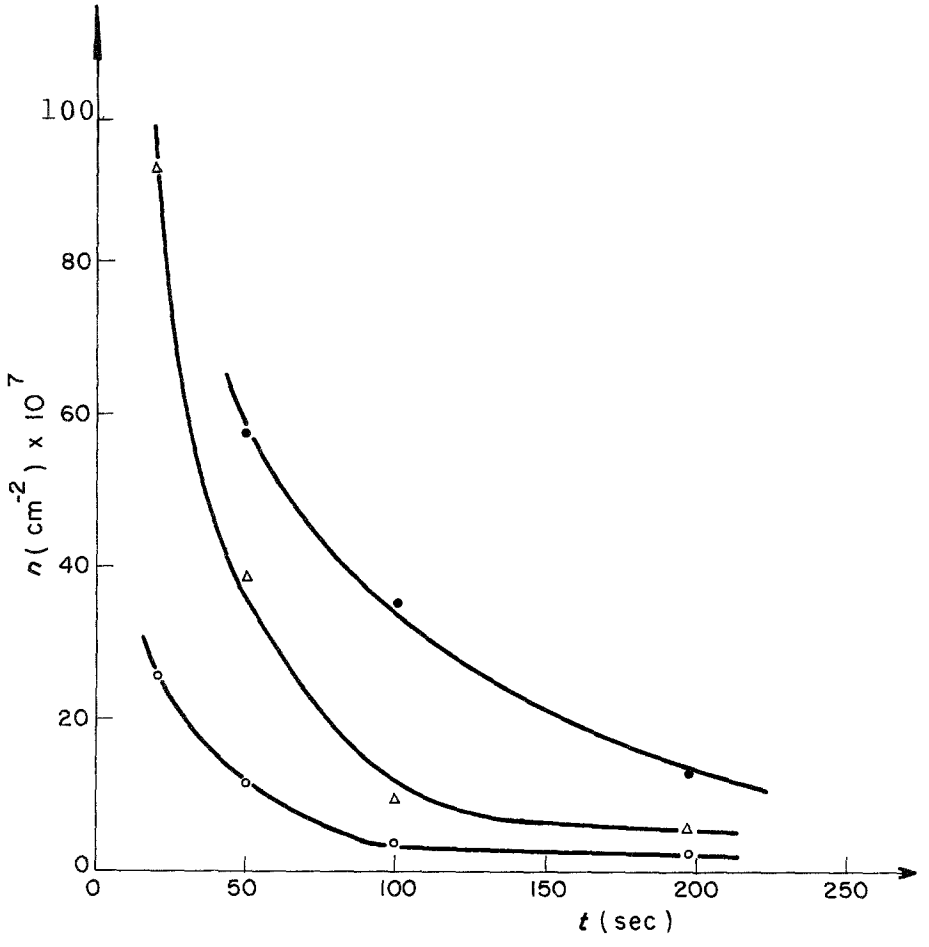

Figure 14 Time dependence of the number density n of selenium particles on a nickel substrate for different substrate temperatures. ○, 60; △, 70; ● 80° C.

TABLE V Experimentally obtained equations for the volumes of selenium films

T(°C)	Substrates			
	Sapphire	Glass	Aluminium	Nickel
60	$8.99 \times 10^{12} \exp(-47.62)t^2$	$69.00 \times 10^{24} \exp(-76.55)t^2$	$56.40 \times 10^{20} \exp(-68.20)t^2$	$15.09 \times 10^{8} \exp(-38.97)t^2$
70	$1.31 \times 10^{12} \exp(-45.84)t^2$	$4.20 \times 10^{24} \exp(-74.82)t^2$	$6.40 \times 10^{20} \exp(-66.51)t^2$	$4.49 \times 10^{8} \exp(-37.64)t^2$
80	$0.18 \times 10^{12} \exp(-44.32)t^2$	$0.24 \times 10^{24} \exp(-72.42)t^2$	$0.43 \times 10^{20} \exp(-64.63)t^2$	$0.65 \times 10^{8} \exp(-36.86)t^2$

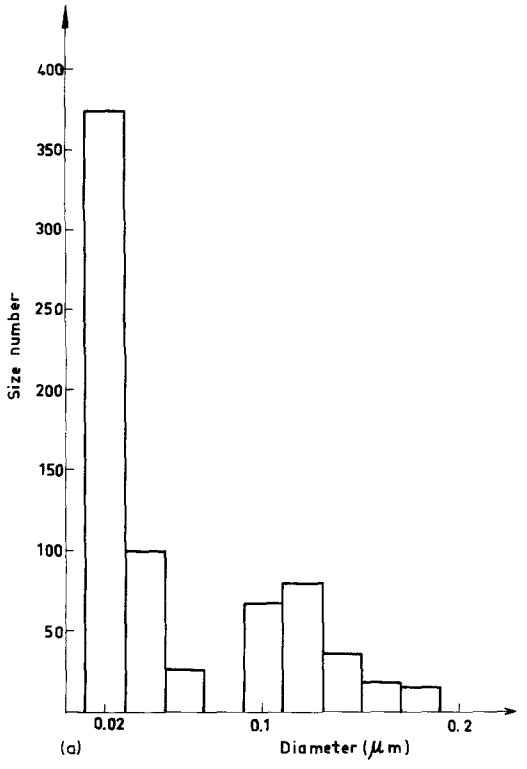

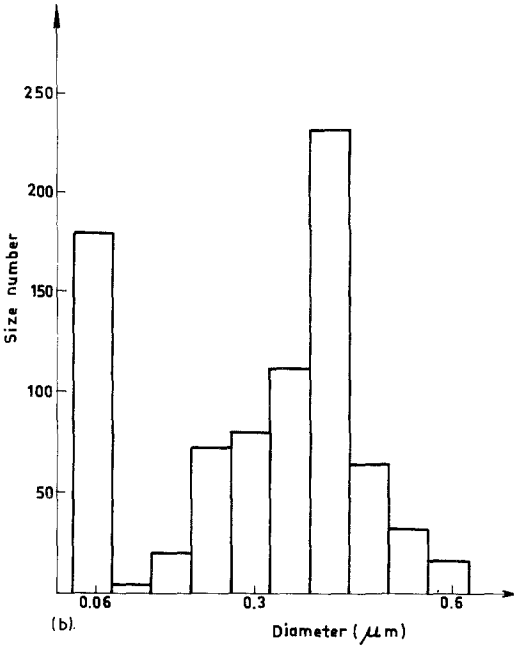

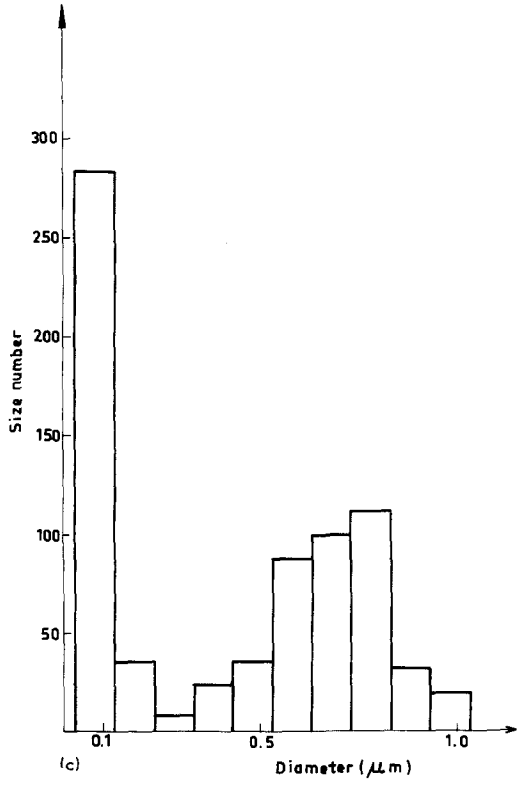

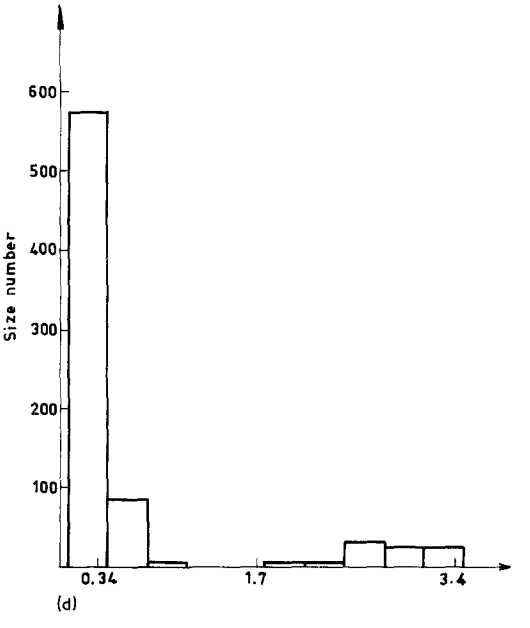

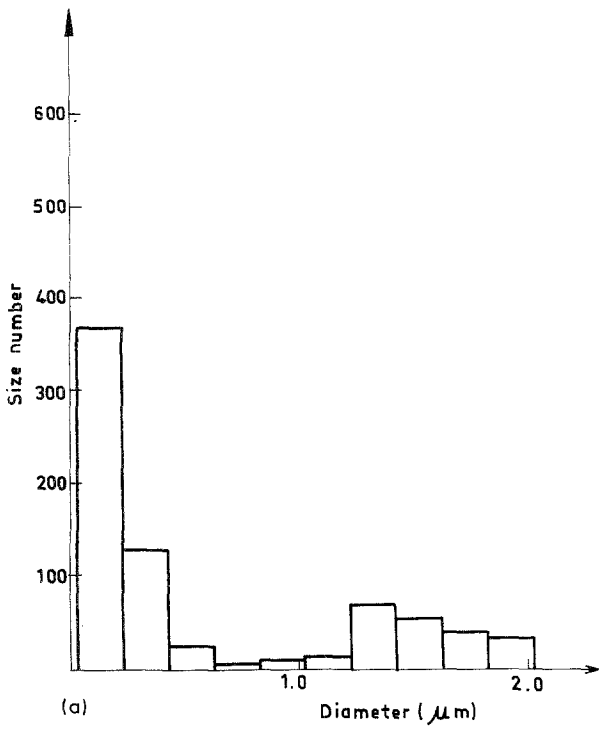

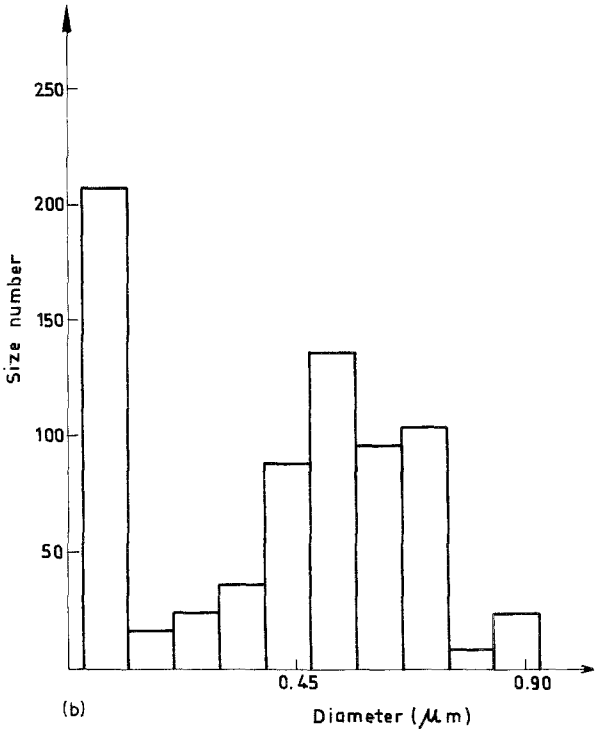

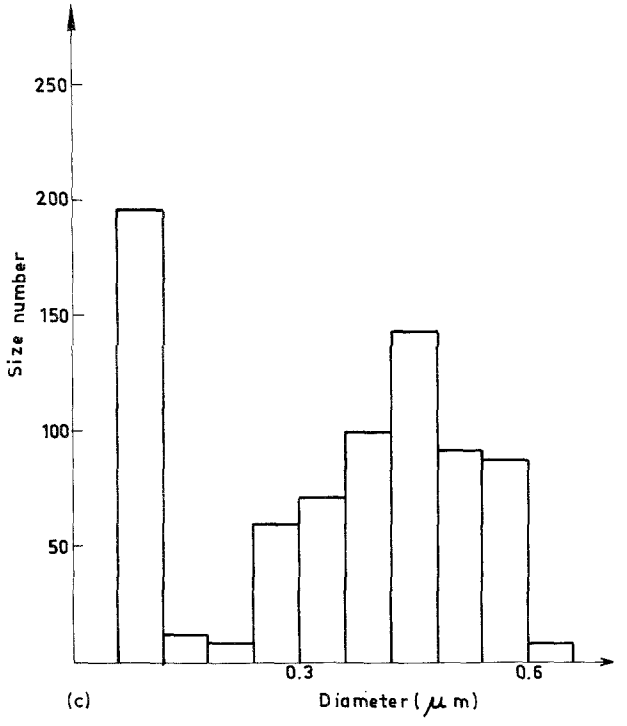

Figure 16 Size distribution histograms of selenium films on the nickel substrate for t = 100 sec. (a) T = 60° C; (b) 70° C; (c) 80° C.

in the present study is a mechanism of the adsorption of impinging selenium atoms on the stable clusters formed on the substrates and the growth of these clusters as evaporation continues. Therefore, the total selenium surface increases with an accompanying increase in the rate of volume growth. However, this rate should follow a constant form after all the substrate surface is covered by a selenium film.

Finally, the pre-exponential factors in Equation 2

TABLE VI Apparent energies for the growth of selenium films on different substrates

Substrate	$\Delta G_{\text{apparent}}$ (eV)
Sapphire	1.36 ± 0.10
Glass	2.20 ± 0.20
Aluminium	1.96 ± 0.15
Nickel	1.12 ± 0.09

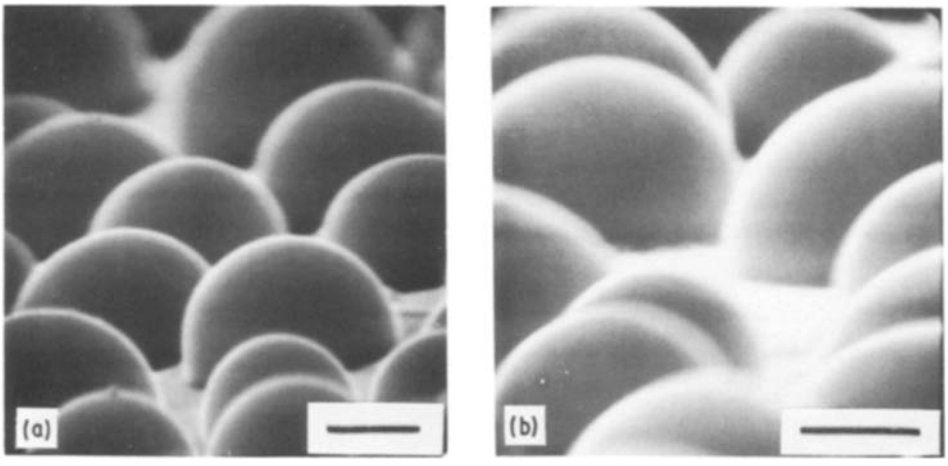

Figure 17 Contact angles in different selenium–substrate systems. (a) Se–Ni system at T = 52° C; (b) Se-sapphire system at T = 90° C. Scale bar, 1 μm.

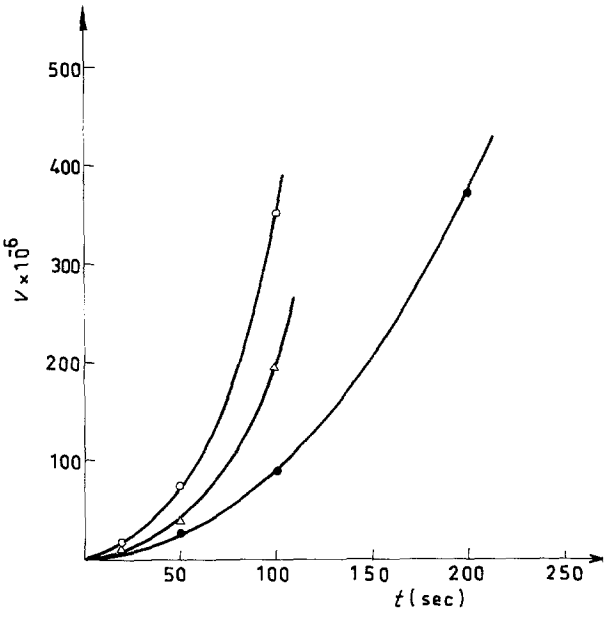

Figure 18 Time dependence of the volume (cm^3/cm^2) of selenium films on a glass substrate for different substrate temperatures. ○, 60; △, 70; ● 80° C.

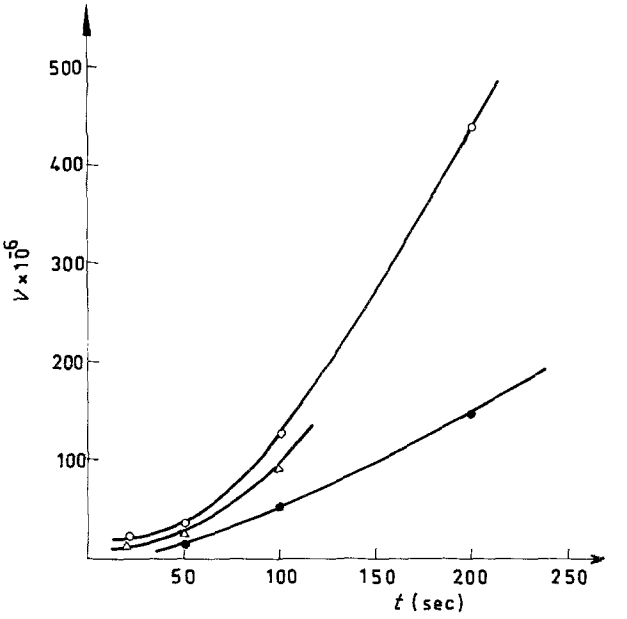

Figure 19 Time dependence of the volume (cm^3/cm^2) of selenium films on an aluminium substrate for different substrate temperatures. ○, 60; △, 70; ● 80° C.

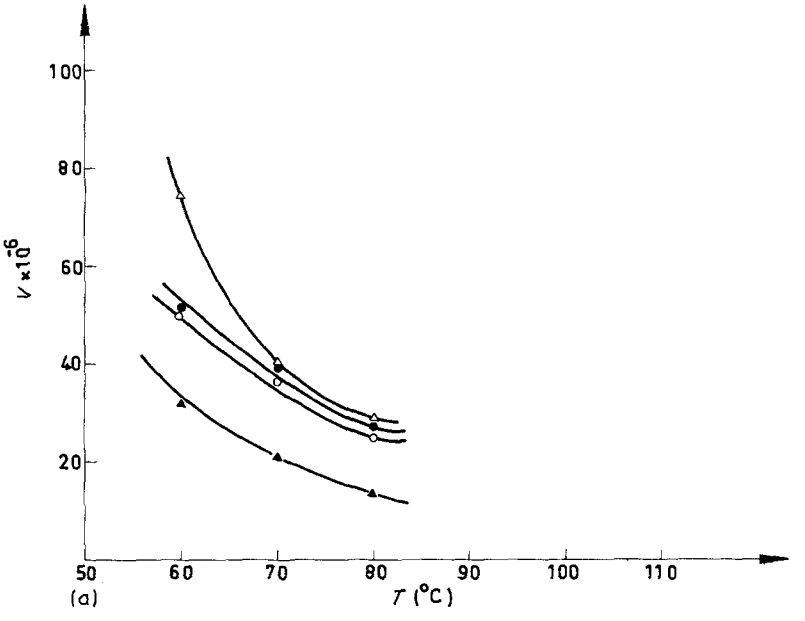

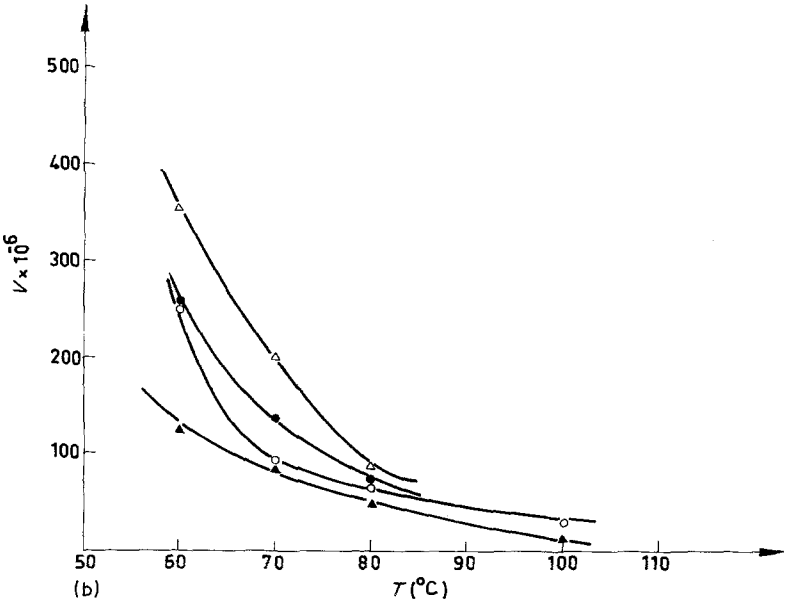

Figure 20 Temperature dependence of the volume (cm^3/cm^2) of selenium films for different substrates. (a) Evaporation time t = 50 sec; (b) t = 100 sec. ○, Sapphire; △, glass; ▲, aluminium; ●, nickel.

will be discussed. The experimentally obtained equations for the volumes of selenium films (Table V) showed that these factors decrease with an accompanying increase in the substrate temperature. This observation can be explained in terms of adatoms re-evaporating from the areas on the substrates which are outside the capture zones around each stable nucleus. Therefore, the pre-exponential factors of Equation 2 are a measure of the difference between the constant deposition flux and the desorption flux which is related to the number of atoms (per unit area per unit time) leaving the substrate surface. The difference between these fluxes at higher temperatures can be explained by the increased probability that an adatom will break its bonds with the substrate surface and incorporate to the vapour phase. At high temperatures, the fractional area of the substrate covered by the selenium islands and their associated capture zones is small due to the re-evaporation of adsorbed atoms. At lower temperatures, however, the probability of the capture of adatoms from the vapour phase to form a stable cluster is more than that of their re-evaporation, and the net flux attains the maximum value.

4. Conclusions

1. The film formation and growth process is thought to be a mechanism of the adsorption of impinging selenium atoms on the stable clusters, and the growth of these clusters as evaporation continues.

2. The differences in the values of the activation energies for the growth of selenium films are explained by considering them as apparent energies which contain the adsorption, desorption, surface diffusion and binding energy terms.

3. The time dependency of Equation 2 was found as t^2 for each substrate. This is explained by the adsorption of selenium atoms on the islands, rather than on the substrates which caused an increase in the rate of volume growth.

4. The decrease in the pre-exponential factor of Equation 2 with the increase in temperature is explained by the increased re-evaporation of adatoms from the substrates at higher temperatures.

Acknowledgements

The author is grateful to Professor Dr Ertuğrul Atasoy for his valuable suggestions. The author also thanks Mr Cengiz Tan for his help in the experimental part of the work.

References

1. D. WALTON, T. RHODIN and R. W. ROLLINS, *J. Chem. Phys.* **38** (1963) 2698.
2. J. P. HIRTH and G. M. POUND, in "Condensation and Evaporation – Nucleation and Growth Kinetics", "Progress in Materials Science" Vol. 11, edited by B. Chalmers (Pergamon, Oxford, 1963).
3. T. RHODIN and D. WALTON, in "Single Crystal Films", edited by M. Francombe and H. Sato (Pergamon, Oxford, 1964) p. 31.
4. G. M. POUND and H. KARGE, in "Basic Problems in Thin Film Physics", edited by R. Niedermayer and H. Mayer (Vandenhoeck and Ruprecht, Göttingen, 1966) p. 19.
5. G. ZINSMEISTER, *ibid.* p. 33.
6. E. BAUER, A. K. GREEN, K. M. KUNZ and H. POPPA, *ibid.* p. 135.
7. J. P. HIRTH and K. L. MOAZED, in "Physics of Thin Films, Vol. 4", edited by G. Hass and R. E. Thun (Academic Press, New York, 1967) p. 97.
8. B. LEWIS, *Thin Solid Films* **1** (1967) 85.
9. K. L. CHOPRA, in "Thin Film Phenomena" (McGraw-Hill, USA, 1969) p. 137.
10. R. A. SIGSBEE, in "Nucleation", edited by A. C. Zettlemoyer (Marcel Dekker, New York, 1969) p. 151.
11. A. OLIVEI, *J. Cryst. Growth* **26** (1974) 243.
12. I. GUTZOW and I. AVRAMOV, *J. Non-Cryst. Solids* **16** (1974) 128.
13. I. MARKOV and R. KAISCHEW, *Thin Solid Films* **32** (1976) 163.
14. B. LEWIS and V. HALPERN, *J. Cryst. Growth* **33** (1976) 39.
15. E. KRIKORIAN and R. J. SNEED, *Astrophys. Space Sci.* **65** (1979) 129.
16. R. HRACH and V. STARY, *Thin Solid Films* **85** (1981) 285.
17. BR. PETRĖTIS, R. RINKŪNAS and V. FILIPAVIČIUS, *ibid.* **85** (1981) 301.
18. S. STOYANOV and D. KASHCHIEV, in "Current Topics in Materials Science, Vol. 7", edited by E. Kaldis (North-Holland, Amsterdam, 1981) p. 69.
19. R. A. OUTLAW and J. H. HEINBOCKEL, *Thin Solid Films* **108** (1983) 79.
20. R. DIMARTINI and R. LACEY, *J. Chem. Phys.* **79** (1983) 5693.
21. D. KASHCHIEV, *J. Cryst. Growth* **67** (1984) 559.
22. A. KUBILIUS, BR. PETRĖTIS, R. RINKŪNAS and V. FILIPAVIČIUS, *Thin Solid Films* **116** (1984) 131.
23. F. C. M. J. M. VAN DELFT, A. D. VAN LANGEVELD and B. E. NIEUWENHUYS, *ibid.* **123** (1985) 333.
24. M. HARSDORFF and W. JARK, *ibid.* **128** (1985) 79.
25. BR. PETRĖTIS and R. RINKŪNAS, *ibid.* **128** (1985) 269.
26. B. F. USHER, *App. Surf. Sci.* **22/3** (1985) 506.
27. J. SALIK, *J. Appl. Phys.* **57** (1985) 5017.
28. H. P. SINGH and L. E. MURR, *Met. Trans.* **3** (1972) 983.
29. M. ÖZENBAŞ, Ph.D. Thesis, Middle East Technical University, Ankara, Turkey, 1981.
30. R. A. SIGSBEE and G. M. POUND, *Adv. Coll. Interf. Sci.* **1** (1967) 335.
31. I. S. GOLDSTEIN, *Thin Solid Films* **39** (1976) 195.

Received 19 May
and accepted 4 September 1986